PREPARED FOR THE U.S. DEPARTMENT OF ENERGY,
UNDER CONTRACT DE-AC02-76-CHO-3073

PPPL-2920
UC-420,421,426,427

PPPL-2920

ACCESSIBILITY FOR LOWER HYBRID WAVES IN PBX-M

BY

H. TAKAHASHI, S. BATHA, R. BELL, ET AL.

JULY, 1993

PRINCETON
PLASMA PHYSICS
LABORATORY

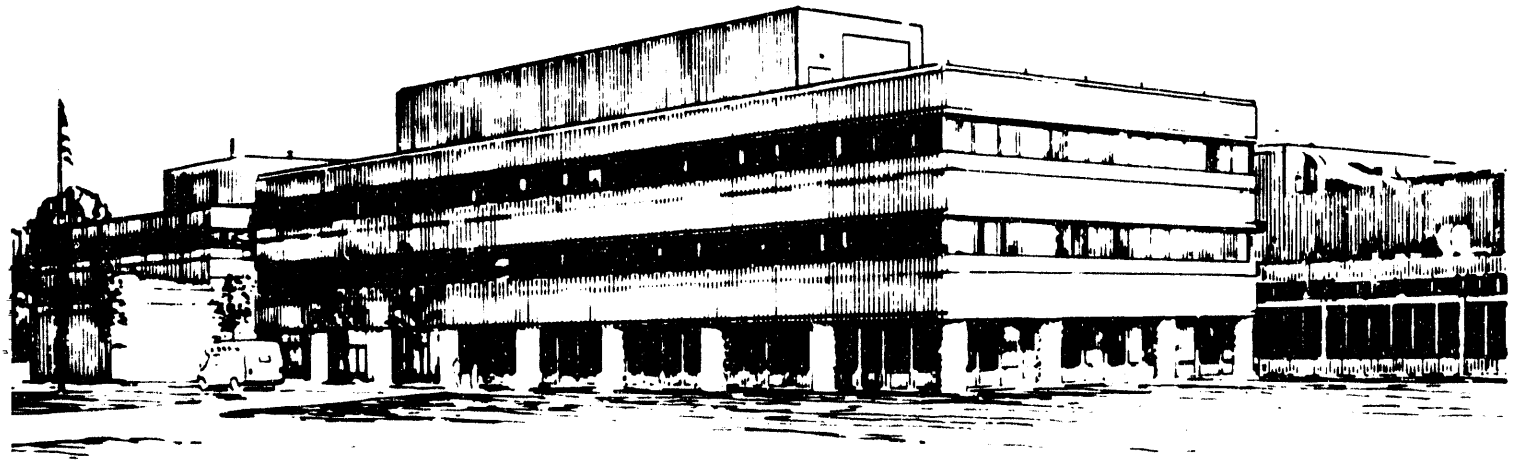

NOTICE

ACCESSIBILITY FOR LOWER HYBRID WAVES IN PBX-M[1]

H. Takahashi, S. Batha[1], R. Bell, S. Bernabei, M. Chance, T. K. Chu, J. Dunlap[2], A. England[2], G. Gettelfinger, N. Greenough, J. Harris[2], R. Hatcher, S. Hirshman[2], D. Ignat, R. Isler[2], S. Jardin, S. Jones[3], R. Kaita, S. Kaye, J. Kesner[3], H. Kugel, B. LeBlanc, F. Levinton[1], S. Luckhardt[3], J. Manickam, M. Okabayashi, M. Ono, F. Paoletti[3], S. Paul, F. Perkins, A. Post-Zwicker[2], N. Sauthoff, L. Schmitz[4], S. Sesnic, Y. Sun, W. Tighe, G. Tynan[4], E. Valeo, and S. von Goeler
Plasma Physics Laboratory, Princeton University, Princeton, NJ, USA
([1]Fusion Physics & Technology, [2]ORNL, [3]MIT, [4]UCLA)

Understanding the wave damping mechanism in the presence of a 'spectral gap' is an important issue for the current profile control using Lower Hybrid Current Drive (LHCD). We examine a traditional explanation based upon upshifting of the wave parallel refractive index ($n_{||}$), and find that there can be an upper bound in the $n_{||}$ upshift. The amount of upshift is not sufficient to bridge the spectral gap completely under some PBX-M LHCD conditions. There is experimental evidence, however, that current was driven even under such conditions. Another mechanism is also considered, based upon the 2-D velocity space dynamics coupled with a compound wave spectrum, here consisting of forward- and backward-running waves. The runaway critical speed relative to the phase speeds of these waves plays an important role in this model.

[1]Supported by USDOE Contract No. DE-AC02-76-CHO-3073

ACCESSIBILITY FOR LOWER HYBRID WAVES IN PBX-M[1]

H. Takahashi, S. Batha[1], R. Bell, S. Bernabei, M. Chance, T. K. Chu, J. Dunlap[2], A. England[2], G. Gettelfinger, N. Greenough, J. Harris[2], R. Hatcher, S. Hirshman[2], D. Ignat, R. Isler[2], S. Jardin, S. Jones[3], R. Kaita, S. Kaye, J. Kesner[3], H. Kugel, B. LeBlanc, F. Levinton[1], S. Luckhardt[3], J. Manickam, M. Okabayashi, M. Ono, F. Paoletti[3], S. Paul, F. Perkins, A. Post-Zwicker[2], N. Sauthoff, L. Schmitz[4], S. Sesnic, Y. Sun, W. Tighe, C. Tynan[4], E. Valeo, and S. von Goeler
Plasma Physics Laboratory, Princeton University, Princeton, NJ, USA
([1]Fusion Physics & Technology, [2]ORNL, [3]MIT, [4]UCLA)

The Lower Hybrid Current Drive (LHCD) experiments on the PBX-M tokamak attempt to modify the current profile in order to find high performance operating regimes.[4] Successful current and safety factor (q) profile modification has been reported.[6,7] Transport of LHCD generated fast electrons by MHD activity[7] and by diffusion[2] has been studied. Relationship between current deposition location and MHD behavior has been examined.[1] Understanding the wave damping mechanism in the face of 'spectral gap' is an important issue for the current profile control, and is discussed here. A traditional explanation based upon upshifting[8] of the wave parallel refractive index ($n_{||}$) is examined. Another mechanism is also considered, based upon the 2-D velocity space dynamics coupled with a compound wave spectrum, here consisting of forward- and backward-running waves. The runaway critical speed relative to the phase speeds of these waves plays an important role.

The power spectrum ($P_{LH}(n_{||})$) of the 4.6 GHz 32-waveguide grill,[9] computed by a Brambilla code,[10] is shown in Fig. 1 for several settings of the phase angle between adjacent waveguides. Each phase setting produces a lobe in the positive $n_{||}$ range representing forward waves, and a generally smaller lobe in the negative range representing backward waves. The distance in $n_{||}$ between the lobes is a structural constant of the grill, and is ~ 8.3 here. As a result, the faster the forward waves are, the slower the conjugate backward waves are. The phase speed of forward waves is, however, much faster than the electron thermal speed (v_e) in our experiments (on-axis electron temperature, $T_e(0) \sim 0.8-1.3$ keV), and there is a spectral gap between v_e and the wave speed. In the Landau damping process in the 1-D velocity space, the gap must be filled with a *contiguous* spectrum of waves for the thermal electrons to be brought to resonance with high phase-speed waves. There are also much smaller side lobes. All lobes are narrow ($\Delta n_{||} \leq 0.5$) owing to the large number of waveguides in the grill. This means that our spectrum is not contiguous, even when all lobes are 'mapped' onto the positive $n_{||}$ side, i.e., there are also gaps in the wave spectrum itself.

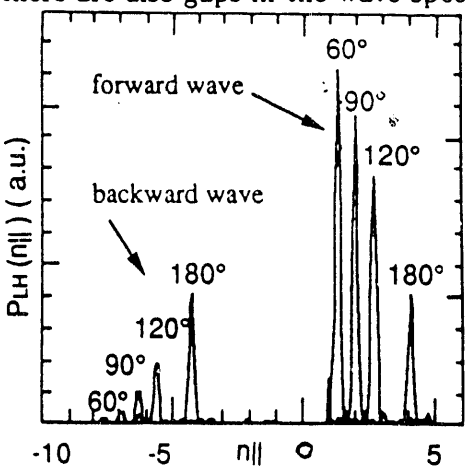

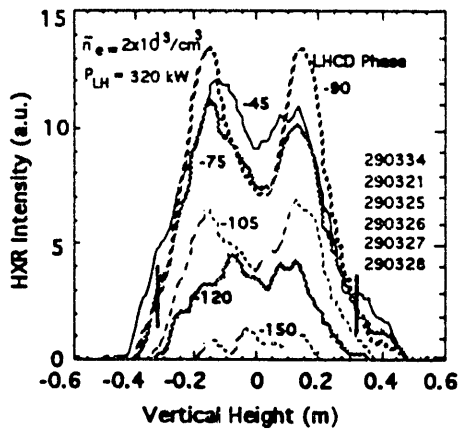

(Left) Fig. 1: An $n_{||}$ spectrum of PBX-M LHCD system; (Right) Fig. 2: A vertical slice of a 2-D HXR camera image through the central region of an ohmically heated bean-shaped plasma. The data was taken in similar discharges over a period 30–45 ms into the LHCD pulse.

A novel 2-D tangentially viewing Hard X-radiation (HXR) camera[3] is used to study the profile of LHCD generated fast electrons. A vertical 'slice' of a 2-D image is shown in Fig. 2 for a series of phases ('phase scan'). Approximate locations of the 'classical' accessibility limit, i.e., the mode conversion point for waves with the grill-imposed $n_{||}^0$, are indicated by short vertical lines on the $-75°$ curve. High phase angles, $-120°$ and $-150°$, are classically accessible to the plasma center. Off-axis peaks were observed for low phase angles up to $-90°$ *inside* the classical accessibility limit. This is evidence that the $n_{||}$ upshift occurred. The peaks appeared

[1]Supported by USDOE Contract No. DE-AC02-76-CHO-3073

at approximately the same location regardless of the phase. But the amplitude of the peaks was strongly dependent on the phase. Theory predicts the current deposition location varying slowly with the phasing (see next paragraph) under conditions for which the $n_{||}$ upshift determines the ultimate wave accessiblity. The experimental results in this respect are not inconsistent with such predictions. But it appears puzzling that more inaccessible low phase angle cases generated a stronger HXR signal.

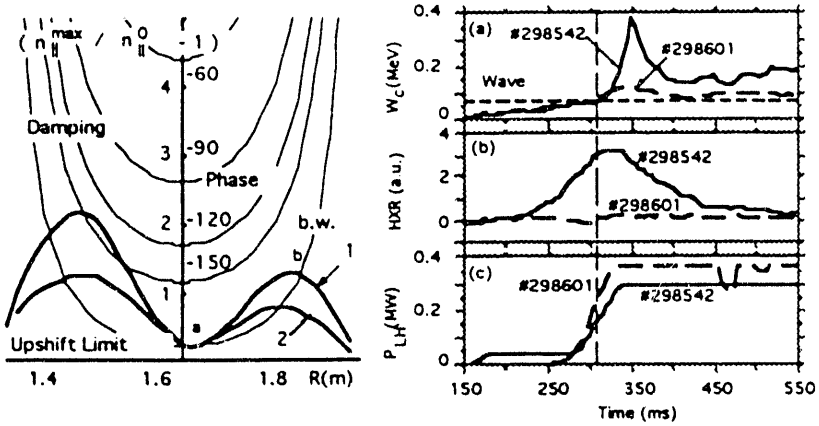

(Left) Fig. 3 Upshift accessibility limit: For profiles the parabola raised to α is used, where α is 1 for n_e and 2 for T_e, $T_e(0)$ is 1 keV. For B_θ/B_ϕ, a model equilibrium with I_p = 180 kA was used; (Right) Fig. 4 Runaway critical energy, HXR from escaping runaways, and LHCD power waveforms.

We first examine the $n_{||}$-upshift caused by toroidal effects. A ray-tracing analysis predicted[5] that, in some cases, especially in bean-shaped plasmas, upshift was sufficient to fill the gap completely and thus to damp the waves. But it predicted also that, in other cases, notably in low density (n_e) circular plasmas, upshift was enough only for the waves to propagate beyond the classical accessibility limit, but not to fill the gap and damp the wave. Inclusion of scattering of the lower hybrid waves by a density turbulence, based upon a theory by Andrews and Perkins,[11] resulted in increased upshift, but the qualitative conclusions remained the same. The upper bound of $n_{||}$ upshift can be estimated by a simple analysis following Kupfer and Moreau.[12] Using the nomenclature of reference[8] and taking the middle two terms of Eq. (15) of that reference, an 'electrostatic' approximation to the dispersion relation is $n_\perp^2 + (n_{||}^2 - \epsilon_\perp)(\epsilon_{||} + \epsilon_\perp)/\epsilon_\perp + \epsilon_{xy}^2/\epsilon_\perp = 0$, where $\epsilon_\perp$, $\epsilon_{||}$, and ϵ_{xy} are the elements of the cold plasma dielectric tensor. We have geometric relationships, ${n_\perp}^2 \approx n_r^2 + n_\theta^2$, $n_{||} \approx n_\phi + n_\theta(B_\theta/B_\phi)$, and $n_\phi = {n_{||}}^0(R_{gr}/R)$, where B_θ and B_ϕ are the azimuthal and toroidal fields, R_{gr} is the grill major radius, and n_r, n_θ and n_ϕ are the radial, azimuthal and toroidal components of the vector refractive index. The value of $n_{||}$ becomes large when n_θ becomes large. The values of n_θ, and hence of $n_{||}$, are at their maximum possible values when $n_r = 0$. We define $g^2 \equiv -(B_\theta/B_\phi)^2(\epsilon_{||} + \epsilon_\perp)/\epsilon_\perp$, and $\alpha \equiv (\epsilon_\perp - \epsilon_{xy}^2/(\epsilon_{||} + \epsilon_\perp))/n_\phi^2$. In the region of interest (where waves propagate) in our experiments, $0 < g^2 < 1$, and $\alpha < 1$. The maximum $n_{||}$ is given by ${n_{||}}^{max}/{n_{||}}^0 = (R_{gr}/R)(1 + \sqrt{1 - (1-g^2)(1+g^2\alpha)})/(1-g^2)$. The expression gives the *upper bound*, and actual 'realizable' values can be lower. In most cases, $g^2 \approx (B_\theta/B_\phi)^2(\omega_{pe}/\omega)^2/(1+(\omega_{pe}/\omega_{ce})^2)$. For $g^2\alpha \ll 1$ the expression simplifies to ${n_{||}}^{max}/{n_{||}}^0 = (R_{gr}/R)/(1 - \mid g \mid)$. The simplified expression yields a universal curve, independent of ${n_{||}}^0$, but overstates the upper bound. The value, ${n_{||}}^{max}/{n_{||}}^0 - 1$, along the mid-plane, using the simple expression is shown in Fig. 3 for the on-axis electron density $n_e(0) = 3{\cdot}10^{19}/m^3$ (Curve 1) and $1.2{\cdot}10^{19}/m^3$ (Curve 2). Shown also in the figure is a series of 'damping' curves whose ordinate is $c/(3v_e{n_{||}}^0) - 1$, where c is the speed of light, indicating for different phases the condition for strong Landau damping (wave speed equals 3–4 times v_e; here 3 is chosen). The curve labeled, 'b.w.,' is for $n_{||} = -6.2$, close to the backward waves of the $-90°$ phase. The waves would damp strongly over the range where the upshift limit curve and a damping curve overlap (e.g., between 'a' and 'b' on the b.w. curve). The 'damping region' would first appear in the mid-radius range, and only gradually expand, as ${n_{||}}^0$ (or T_e or n_e) increases. When the two curves do not intersect, the vertical distance between them represents a spectral gap remaining after maximum upshift is attained. The Curve 1 and damping curves represent approximately the phase scan discussed earlier, showing that the gap existed for all cases except the $-150°$ phase and backward waves. The gap is, however, smallest in the mid-radius region, and current

would be driven there if the gap is bridged by *some* mechanisms. Many other cases, notably low n_e, low current circular plasmas, had a gap similar to, or greater than, those between the Curve 2 and damping curves. Yet, a drop in the loop voltage (V_l) indicated that current was driven. These observations led to the question as to what fills the remaining spectral gap in these cases.

We now compare two nearly identical target discharges in which an LHCD pulse, similar in power, but different in waveform, was applied. The current deposition (inferred from 2-D HXR camera images — not shown) was very different in its spatial profile and time evolution. The LHCD phase was $-90°$ ($n_{||} \sim 2.1$) for the both discharges. In one discharge (#298601) a nearly square waveform pulse was applied, but in the other (#298542) there was a long ($\sim$ 100 ms) low-power ($\sim$ 12 kW) pedestal ahead of the higher-power main pulse. The waveforms are shown in Fig. 4(c). Both discharges had neutral beam injection (NBI) heating over 250−580 ms with an absorbed power ($\sim$ 350 kW) comparable to $P_{LH} \sim 300$ kW. In #298601 the HXR camera image was characterized by persistent 'hollowness' in the center between off-axis peaks. This implies sustained localization of off-axis current drive, a desirable characteristic for current profile control. In #298542 the profile was centrally peaked and rapidly grew toward its maximum value. Most of the rise occured *during the low-power pedestal.* The HXR emission produced by escaping runaway electrons was monitored by a scintilator. We examine its signals shown in Fig. 4(b) in the early part of the LHCD pulse. The background level was removed from either data by using the signal from a third discharge (#298559 — not shown) that had only NBI heating, but no LHCD. There was no increase in the scintilator signal attributable to LHCD for #298601. There was a rapid increase, after a delay ($\sim$ 50 ms), of the signal during the pedestal for #298542. The minimal power that caused the signal rise suggests that the process was probably not limited by the availability of the wave power. The critical energy (W_c) for a test electron to runaway in the presence of an electric field (E) is plotted in Fig. 4(a). The critical energy here is the value computed from Eq. (2.13) of Knoepfel and Spong[16] times $(2+Z_{eff})/3$, where Z_{eff} is the effective ionic charge. The density representative of mid-radius regions was used. The value, $Z_{eff} = 4$, was assumed for these target discharges which had a relatively high loop voltage ($V_l \sim 1.5V$). Shown also in the figure is the energy corresponding to $n_{||}{}^0$. The W_c values are below the wave 'energy' for the both discharges initially, indicating that, *if* there are electrons with energies beyond the runaway critical energy, E field can cause them to runaway. Since the target discharges were not runaway discharges, it is likely that the waves carried thermal electrons to the runaway critical energy. In many other situations, small changes in plasma parameters, notably V_l and n_e, often resulted in a very different current deposition profile and evolution. This 'volatility' of the results does not appear to be amenable to an easy explanation in terms of the wave propagation characteristics, such as *changes* in the classical or upshifted accessibility limit.

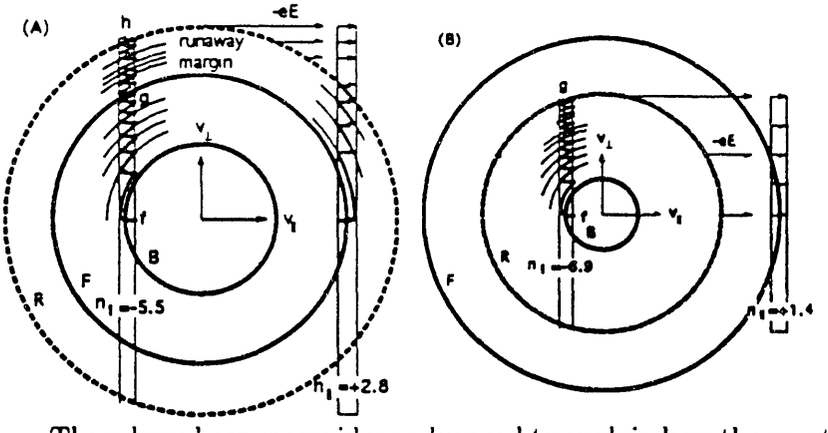

Fig. 5: (A) Runaway critical energy greater than either wave phase speed. The backward waves can feed electrons to the forward and upshifted waves; (B) Runaway critical energy intervenes between the wave phase speeds. The backward waves do not feed electrons to the forward waves, but to runaway population.

There have been many ideas advanced to explain how the spectral gap may be bridged. They include an extension of the imposed wave spectrum to higher $n_{||}$ values by some unspecified mechanisms, and additional upshift due to some causes other than toroidal effects. We consider here effects of the backward waves. The model is of speculative nature and needs quantitative computational verification and further experimental tests. Electrons can gain speed beyond

the wave speed under the combined influence of lower hybrid waves and pitch angle scattering. This 2-D mechanism was studied intensively following a publication by Karney and Fisch.[13] In the presence of low phase-speed backward waves, the mechanism may serve as a means of supplying fast electrons to higher phase-speed forward waves. In the wave resonance zones, represented by a pair of vertical lines in Fig. 5 (A), electrons are accelerated by the wave field, and are then distributed along constant energy circles through pitch angle scattering. Two solid line circles, F and B, represent such a trajectory passing through the phase speed of the forward and backward waves, respectively. Those electrons, that gain speed from the backward waves and reach a point between f and g, can pitch angle scatter and interact with upshifted forward waves, and those that reach a point beyond g can resonate with the forward waves. The dashed line circle, R, represents a critical energy for electrons to runaway with a substantial probability in the presence of an E field (the boundary shape is in detail not a simple circle[14]). Those electrons, that reach h can become runaways, but the number of such electrons is small, when the 'runaway margin,' i.e., the distance between F and R, is large. In this model, it is crucial whether R is beyond both F and B as shown in (A), or R intervenes between F and B as shown in (B). Now, referring to (B), those electrons, that reach g can become runaways. The runaways can interact with the forward waves, but the forward waves are now rendered irrelevant, because the electrons continue to gain speed from the field. (Appert, et al.[18] has shown that a strong enhancement of the runaway production can occur through the 2-D dynamics.) Owing to the difference in the wave phase speeds, those electrons resonant with the backward waves are exponentially more numerous, and suffer far more frequent pitch angle scattering, compared to those electrons resonant with the forward waves. An inspection of the shape of the velocity space 'stream lines' computed by Karney and Fisch[13] shows that the bulk of the particle flux moves in the direction opposite the waves, and suggests that the backward waves may be effective in supplying electrons to the forward waves. (In a so-called compound wave spectrum[17] the high $n_{||}$ *forward* waves can play a similar role.) It is the electrons that fill up the spectral gap in this model, rather than a contiguous spectrum of waves, although the $n_{||}$ upshift of both the forward and backward waves also play an important role in bridging the gap. The runaway critical speed ($\propto n_e/E$), relative to the forward wave speed, can change quickly during a discharge, depending upon how far and quickly E is depressed by the current drive, and how n_e evolves. This may be a reason for the sensitivity of our current profile control experiments to date. Tailoring the waveform during the discharge may be useful, not only of the LHCD power, but also of the phase setting, taking advantage of the PBX-M LHCD system capability for rapid phase change.[9] Recently, Colborn, et al.[19] considered, based in part on CQL3D code results, broad side-lobes and backward lobes that would bridge the full extent of the spectral gap contiguously. In such a situation, only pitch angle scattering along constant energy circles, but not the acceleration mechanism, is required to bridge the gap.

In summary, some observations made in our experiments are not readily explainable in terms of the conventional theory based upon $n_{||}$ upshift. A simple theoretical analysis indicates that there is an upper bound in $n_{||}$, and there are spectral gaps that cannot be bridged by the $n_{||}$ upshift caused by toroidal effects alone. We are exploring a possible explanation in terms of the backward waves. Other explanations are also being considered.

We thank Dr. P. Bonoli and Dr. R. Harvey for bringing to our attention during the preparation of this manuscript the existence of a work[19] by Dr. J. Colborn, et al.

REFERENCES : **(1)** R. Bell, 10th Topical Conf. on Radio Frequency Power in Plasmas, Boston, 1993, Invited Paper; **(2)** S. Jones, *ibid*, Paper C13; **(3)** S. von Goeler, et al., *ibid*, Paper C14; **(4)** M. Okabayashi, et al., *ibid*, Paper C15; **(5)** D. Ignat, *ibid*, Paper C16; **(6)** R. Kaita, et al, IAEA, Würzburg, 1992; **(7)** S. Bernabei, et al., Invited Paper, APS Meeting, 1992; **(8)** P. Bonoli and R. Englade, Phys. Fluids, **29**(1986)2937; **(9)** N. Greenough, et al., 14th IEEE/NPSS Symp. on Fusion Eng., Vol. 1, p126, 1991; **(10)** M. Brambilla, Nucl. Fusion, **16**(1976)47; **(11)** Andrews and Perkins, Phys. Fluids **26**(1983)2537; **(12)** Kupfer and Moreau, Nucl. Fusion, **32**(1992)1845; **(13)** C. Karney and N. Fisch, Phys. of Fluids, **22**(1979)1817; **(14)** Karney and N. Fisch, Phys. of Fluids, **29**(1986)180; **(15)** J. Kesner, MIT Report PFC/JA-92-24, 1993; **(16)** H. Knoepfel and D. Spong, Nucl. Fusion, **19**(1979)785; **(17)** F. Soeldner, et al.,IAEA Washingon, 1990; **(18)** K. Appert, et al., EPS Conference, Aachen, p329, 1983; **(19)** J. Colborn, et al., submitted to Phys. Fluids.

EXTERNAL DISTRIBUTION IN ADDITION TO UC-420

Dr. F. Paoloni, Univ. of Wollongong, AUSTRALIA
Prof. M.H. Brennan, Univ. of Sydney, AUSTRALIA
Plasma Research Lab., Australian Nat. Univ., AUSTRALIA
Prof. I.R. Jones, Flinders Univ, AUSTRALIA
Prof. F. Cap, Inst. for Theoretical Physics, AUSTRIA
Prof. M. Heindler, Institut für Theoretische Physik, AUSTRIA
Prof. M. Goossens, Astronomisch Instituut, BELGIUM
Ecole Royale Militaire, Lab. de Phy. Plasmas, BELGIUM
Commission-European, DG. XII-Fusion Prog., BELGIUM
Prof. R. Boucique, Rijksuniversiteit Gent, BELGIUM
Dr. P.H. Sakanaka, Instituto Fisica, BRAZIL
Instituto Nacional De Pesquisas Espaciais-INPE, BRAZIL
Documents Office, Atomic Energy of Canada Ltd., CANADA
Dr. M.P. Bachynski, MPB Technologies, Inc., CANADA
Dr. H.M. Skarsgard, Univ. of Saskatchewan, CANADA
Prof. J. Teichmann, Univ. of Montreal, CANADA
Prof. S.R. Sreenivasan, Univ. of Calgary, CANADA
Prof. T.W. Johnston, INRS-Energie, CANADA
Dr. R. Bolton, Centre canadien de fusion magnétique, CANADA
Dr. C.R. James,, Univ. of Alberta, CANADA
Dr. P. Lukác, Komenského Universzita, CZECHO-SLOVAKIA
The Librarian, Culham Laboratory, ENGLAND
Library, R61, Rutherford Appleton Laboratory, ENGLAND
Mrs. S.A. Hutchinson, JET Library, ENGLAND
Dr. S.C. Sharma, Univ. of South Pacific, FIJI ISLANDS
P. Mähönen, Univ. of Helsinki, FINLAND
Prof. M.N. Bussac, Ecole Polytechnique,, FRANCE
C. Mouttet, Lab. de Physique des Milieux Ionisés, FRANCE
J. Radet, CEN/CADARACHE - Bat 506, FRANCE
Prof. E. Economou, Univ. of Crete, GREECE
Ms. C. Rinni, Univ. of Ioannina, GREECE
Dr. T. Mual, Academy Bibliographic Ser., HONG KONG
Preprint Library, Hungarian Academy of Sci., HUNGARY
Dr. B. DasGupta, Saha Inst. of Nuclear Physics, INDIA
Dr. P. Kaw, Inst. for Plasma Research, INDIA
Dr. P. Rosenau, Israel Inst. of Technology, ISRAEL
Librarian, International Center for Theo Physics, ITALY
Miss C. De Palo, Associazione EURATOM-ENEA , ITALY
Dr. G. Grosso, Istituto di Fisica del Plasma, ITALY
Prof. G. Rostangni, Istituto Gas Ionizzati Del Cnr, ITALY
Dr. H. Yamato, Toshiba Res & Devel Center, JAPAN
Prof. I. Kawakami, Hiroshima Univ., JAPAN
Prof. K. Nishikawa, Hiroshima Univ., JAPAN
Director, Japan Atomic Energy Research Inst., JAPAN
Prof. S. Itoh, Kyushu Univ., JAPAN
Research Info. Ctr., National Instit. for Fusion Science, JAPAN
Prof. S. Tanaka, Kyoto Univ., JAPAN
Library, Kyoto Univ., JAPAN
Prof. N. Inoue, Univ. of Tokyo, JAPAN
Secretary, Plasma Section, Electrotechnical Lab., JAPAN
S. Mori, Technical Advisor, JAERI, JAPAN
Dr. O. Mitarai, Kumamoto Inst. of Technology, JAPAN
J. Hyeon-Sook, Korea Atomic Energy Research Inst., KOREA
D.I. Choi, The Korea Adv. Inst. of Sci. & Tech., KOREA
Prof. B.S. Liley, Univ. of Waikato, NEW ZEALAND
Inst of Physics, Chinese Acad Sci PEOPLE'S REP. OF CHINA
Library, Inst. of Plasma Physics, PEOPLE'S REP. OF CHINA
Tsinghua Univ. Library, PEOPLE'S REPUBLIC OF CHINA
Z. Li, S.W. Inst Physics, PEOPLE'S REPUBLIC OF CHINA
Prof. J.A.C. Cabral, Instituto Superior Tecnico, PORTUGAL
Dr. O. Petrus, AL I CUZA Univ., ROMANIA
Dr. J. de Villiers, Fusion Studies, AEC, S. AFRICA
Prof. M.A. Hellberg, Univ. of Natal, S. AFRICA
Prof. D.E. Kim, Pohang Inst. of Sci. & Tech., SO. KOREA
Prof. C.I.E.M.A.T, Fusion Division Library, SPAIN
Dr. L. Stenflo, Univ. of UMEA, SWEDEN
Library, Royal Inst. of Technology, SWEDEN
Prof. H. Wilhelmson, Chalmers Univ. of Tech., SWEDEN
Centre Phys. Des Plasmas, Ecole Polytech, SWITZERLAND
Bibliotheek, Inst. Voor Plasma-Fysica, THE NETHERLANDS
Asst. Prof. Dr. S. Cakir, Middle East Tech. Univ., TURKEY
Dr. V.A. Glukhikh,Sci. Res. Inst. Electrophys.I Apparatus, USSR
Dr. D.D. Ryutov, Siberian Branch of Academy of Sci., USSR
Dr. G.A. Eliseev, I.V. Kurchatov Inst., USSR
Librarian, The Ukr.SSR Academy of Sciences, USSR
Dr. L.M. Kovrizhnykh, Inst. of General Physics, USSR
Kernforschungsanlage GmbH, Zentralbibliothek, W. GERMANY
Bibliothek, Inst. Für Plasmaforschung, W. GERMANY
Prof. K. Schindler, Ruhr-Universität Bochum, W. GERMANY
Dr. F. Wagner, (ASDEX), Max-Planck-Institut, W. GERMANY
Librarian, Max-Planck-Institut, W. GERMANY
Prof. R.K. Janev, Inst. of Physics, YUGOSLAVIA

END

DATE FILMED

9/2/93